Kinetics of phase separation in thin films: Lattice versus continuum models for solid binary mixtures

Subir K. Das,[1] Jürgen Horbach,[2] and Kurt Binder[3]

[1]*Theoretical Sciences Unit, Jawaharlal Nehru Centre for Advanced Scientific Research, Jakkur, Bangalore 560064, India*
[2]*Institut für Materialphysik im Weltraum, Deutsches Zentrum für Luft- und Raumfahrt (DLR), 51170 Köln, Germany*
[3]*Institut für Physik, Johannes Gutenberg-Universität Mainz, Staudinger Weg 7, 55099 Mainz, Germany*

A description of phase separation kinetics for solid binary (A,B) mixtures in thin film geometry based on the Kawasaki spin-exchange kinetic Ising model is presented in a discrete lattice molecular field formulation. It is shown that the model describes the interplay of wetting layer formation and lateral phase separation, which leads to a characteristic domain size $l(t)$ in the directions parallel to the confining walls that grows according to the Lifshitz-Slyozov $t^{1/3}$ law with time t after the quench. Near the critical point of the model, the description is shown to be equivalent to the standard treatments based on Ginzburg-Landau models. Unlike the latter, the present treatment is reliable also at temperatures far below criticality, where the correlation length in the bulk is only of the order of a lattice spacing, and steep concentration variations may occur near the walls, invalidating the gradient square approximation. A further merit is that the relation to the interaction parameters in the bulk and at the walls is always transparent, and the correct free energy at low temperatures is consistent with the time evolution by construction.

I. INTRODUCTION

A basic problem of both materials science [1,2] and statistical mechanics of systems out of equilibrium [2–5] is the process of spinodal decomposition of binary (A,B) mixtures. When one brings the system by a sudden change of external control parameters (e.g., a temperature quench) from an equilibrium state in the one-phase region of the mixture to a state inside of the miscibility gap, thermal equilibrium requires coexistence of macroscopically large regions of A-rich and B-rich phases. Related phenomena also occur in systems undergoing order-disorder phase transitions, and it is also possible that an interplay of ordering and phase separation occurs, particularly in metallic alloys with complex phase diagrams [1,2,6].

The recent interest in nanostructured materials and thin films has led to consider the effects of walls or free surfaces on the kinetics of such phase changes [7–19]. In a binary mixture, it is natural to expect that one of the components (say, A) will be preferentially attracted to the surface. Already in the one phase region, this attraction will lead to the formation of surface enrichment layers of the preferred component at the walls, but the thickness of these layers will be small, viz., of the order of the correlation length ξ of concentration fluctuations in the mixture [20]. Only near the critical point this surface enrichment becomes long ranged [21,22]. For temperatures below the critical point, however, the behavior is more complicated due to the interplay between bulk phase separation and wetting phenomena [23–29]. In a semi-infinite geometry, a B-rich domain of a phase separated mixture would be coated with an A-rich wetting layer at the surface, if the temperature is above the wetting transition. Of course, for thin films the finite film thickness D also constrains the growth of wetting layers: E.g., for short-range forces between the walls and the A atoms the equilibrium thickness of a "wetting layer" is of the order of

$\xi \ln(D/\xi)$ [29–31], while at lower temperatures where the surface is nonwet the thickness of the surface enrichment layer again only is of the order of ξ. Also the phase diagram of the system in a thin film geometry differs from that of the bulk, in analogy to capillary condensation of fluids [29,31–34], and very rich phase diagrams may occur, in particular, if the surfaces confining the thin film are not of the same type [29,35–37]. These changes in the phase behavior of thin films are reflected in the kinetics of phase separation in these systems [18,19], of course.

Despite the large theoretical activity on surface effects on phase separation kinetics [8–10,12–15,17–19] the applicability of these works on experiments is very restricted. Actually, most of the experiments deal with thin films of fluid binary mixtures [7,11,16], but almost all theoretical works [8–10,12–15,17,18] deal with "model B" [38], where hydrodynamic interactions are neglected, and hence this model is really appropriate only for solid mixtures.

A second restriction on the applicability of the theory is the fact that it is based on the time-dependent Ginzburg-Landau model [1–6], and thus is applicable only when the correlation length ξ is very large, i.e., in the immediate vicinity of the bulk critical point. For a thin film with short-range surface forces, the "standard model" is based on a free energy functional of an order parameter ψ, and this functional consists of a bulk term (F_b) and two terms representing the two surfaces $\mathcal{S}1$, $\mathcal{S}2$ [8,10,12–14,17,18], $F[\psi]=F_b+F_{\mathcal{S}1}+F_{\mathcal{S}2}$, with

$$F_b[\psi] = \int d\vec{r} \left\{ -\frac{\psi(\vec{r})^2}{2} + \frac{\psi(\vec{r})^4}{4} + \frac{1}{4}[\vec{\nabla}\psi(\vec{r})]^2 \right\}, \quad (1)$$

$$F_{\mathcal{S}1} = \int_{\mathcal{S}1} d\vec{\rho} \left\{ -\frac{g}{2}[\psi(\vec{\rho},0)]^2 - h_{\mathcal{S}1}\psi(\vec{\rho},0) - \gamma\psi(\vec{\rho},0) \right.$$

$$\left. \times \left. \frac{\partial\psi}{\partial z}\right|_{z=0} \right\}, \qquad (2)$$

$$F_{\mathcal{S}2} = \int_{\mathcal{S}2} d\vec{\rho} \left\{ -\frac{g}{2}[\psi(\rho,D)]^2 - h_{\mathcal{S}2}\psi(\vec{\rho},D) + \gamma\psi(\vec{\rho},D) \right.$$

$$\left. \times \left. \frac{\partial\psi}{\partial z}\right|_{z=D} \right\}. \qquad (3)$$

Here $\psi(\vec{r})$ is the order parameter which is proportional to the density difference between the two species; it is normalized such that the coexisting A-rich and B-rich bulk phases for temperature $T < T_{cb}$ (T_{cb} being the bulk critical temperature) correspond to $\psi = \pm 1$, respectively. All lengths are measured in units of 2ξ, with ξ denoting the bulk correlation length at the coexistence curve. The terms $F_{\mathcal{S}1}$ and $F_{\mathcal{S}2}$ are the local contributions from the surfaces $\mathcal{S}1$ and $\mathcal{S}2$, which for a film of thickness D, are located at $z=0$ and $z=D$, respectively, orienting the z axis perpendicular to the surfaces, while $\vec{\rho}$ denotes the $(d-1)$ coordinates parallel to the surfaces, d being the dimensionality. In $F_{\mathcal{S}1}$ there are parameters g, γ, and $h_{\mathcal{S}1}$, which can be related to the temperature T and various parameters of an Ising ferromagnet with a free surface at which a surface magnetic field $H_{\mathcal{S}1}$ acts [8,39]

$$h_{\mathcal{S}1} = 4(H_{\mathcal{S}1}/T)(\sqrt{12})^3\xi^5/\sqrt{3},$$

$$g = 8(4J_s/J - 5)\xi^4,$$

$$\gamma = 4\xi^3, \qquad (4)$$

with

$$\xi = \frac{1}{\sqrt{12}}\left[1 - \frac{T}{T_{cb}}\right]^{-1/2}, \quad k_BT_{cb} = 6J. \qquad (5)$$

In Eqs. (4) and (5), a simple cubic lattice was assumed, the z axis coinciding with a lattice axis. Nearest-neighbor Ising spins in the lattice interact with an exchange coupling J, except for the surface plane at $z=0$ where the exchange coupling is J_S. For deriving Eqs. (1) and (2) from a layerwise molecular field approximation, the limit $\xi \to \infty$ needs to be taken, with $\psi(\vec{\rho},z) = m_n(\vec{\rho},t)/m_b$, where n is the layer index of the lattice, $n=1$ being the surface plane, and m_b $[=\sqrt{3}(1-T/T_{cb})^{1/2}]$ the bulk magnetization (note that $m_b \to 0$ in the considered limit). Finally, $F_{\mathcal{S}2}$ describes analogously, the surface free energy of the surface at $z=D$, with $h_{\mathcal{S}2}$ being related to the surface field $H_{\mathcal{S}2}$ analogously to Eq. (4). In Eq. (5), ξ is measured in units of the lattice spacing a of the molecular field lattice model, which often, for the sake of convenience, we set to 1.

Dynamics is associated to the model assuming that in the bulk the order parameter evolves according to the (nonlinear) Cahn-Hilliard equation [1–6]

$$\frac{\partial}{\partial\tau}\psi(\vec{r},\tau) = -\vec{\nabla}\cdot\vec{J}(\vec{r},\tau) = \vec{\nabla}\cdot\left[\vec{\nabla}\left(\frac{\delta F}{\delta\psi}\right)\right], \qquad (6)$$

while the surfaces amount to two boundary conditions each [20], which can be written as

$$\tau_0\frac{\partial}{\partial\tau}\psi(\vec{\rho},0,\tau) = -\frac{\delta\mathcal{F}}{\delta\psi(\vec{\rho},0,\tau)} = h_{\mathcal{S}1} + g\psi(\vec{\rho},0,\tau) + \gamma\left.\frac{\partial\psi}{\partial z}\right|_{z=0}, \qquad (7)$$

$$J_z(\vec{\rho},0,\tau) = -\frac{\partial}{\partial z}\left[-\psi + \psi^3 - \frac{1}{2}\nabla^2\psi\right] = 0. \qquad (8)$$

Equation (7) describes a nonconserved relaxation ("model A" [38]) for the order parameter at the surface, τ_0 setting the time scale. Since $\psi(\vec{\rho},0,\tau)$ relaxes much faster than the time scales of phase separation away from the surface, one may put $\tau_0 = 0$. The equations for $z=D$ are fully analogous to those for $z=0$. We emphasize that Eq. (6) can also be derived [40] from a continuum approximation to a molecular field approximation to a description of a Kawasaki kinetic Ising model [41], and Eqs. (7) and (8) can be derived from a Kawasaki model with a free surface as well [20]. However, it is clear that the model, Eqs. (6)–(8), can only represent the molecular field Kawasaki kinetic Ising model accurately when $\xi \gg$ one lattice unit. This fact was already discussed in Ref. [20] in the one-phase region, where the linearized molecular field equations on the lattice were solved to describe the kinetics of surface enrichment for $T > T_{cb}$, and it was found that the lattice and continuum theories agree when approximations such as $\exp(-1/\xi) \simeq 1 - 1/\xi$ become valid.

Thus, the model Eqs. (6)–(8) can describe a solid binary mixture accurately near the bulk critical point only: far below T_{cb}, terms of order ψ^6 and higher would be needed in Eq. (1) already, and when ξ is of the order of the lattice spacing a, also higher order gradient terms $(\vec{\nabla}^2\psi)^2$, etc., would be required for an accurate continuum description. However, the numerical solutions of Eqs. (6)–(8) require a discretization anyway: Often a mesh size $\Delta x = \Delta y = \Delta z = 1$ is used to solve these equations [8,10,12–14,17,18]. This essentially corresponds to a lattice with spacing 2ξ, rather than the spacing a of the underlying Ising lattice. Having in mind applications of the theory at temperatures that are not close to the critical point, however, ξ is of the order of 1.

Recently, it was pointed out [42,43] that the quantitatively accurate solution of Eqs. (1)–(6) requires a careful consideration of the interplay of the boundary condition at the wall with the mesh size of the discretization Δz in the direction perpendicular to the wall. For an accurate treatment of the continuum limit of the discretization of the differential equation, Eq. (6), a mesh size $\Delta z \ll 1$ is needed, requiring a different formulation than simply discretizing Eqs. (7) and (8), while the discretization of Eqs. (7) and (8) is appropriate if the lattice spacing is used as a grid spacing [43]; however, the numerical solution of this (commonly used [8,10,12–14,17,18]) discretized model does not correspond accurately to the continuum model, and the question then naturally arises under which conditions it is an accurate approximation to the underlying lattice model, on which the

identification of the parameters in Eqs. (4) and (5) was based.

In Ref. [20], this question was only considered in the simple (analytically soluble) case where all nonlinear terms in the order parameter field were neglected. In view of the criticism of Refs. [42,43], it is unclear whether the commonly used model of surface-directed spinodal decomposition [8,10,12–14,17,18] becomes a quantitatively accurate description of its underlying microscopic model or not. Of course, a clarification of this issue is desirable, and this is one of the purposes of the present paper.

Thus, it is plausible that one could solve with a comparable effort the original (nonlinear) molecular field equations for the Kawasaki kinetic Ising model on the lattice, that are underlying this theory. The advantage of such a treatment clearly would be that the model has a well-defined microscopic meaning at all temperatures. Near the critical temperature, the results of this treatment should become indistinguishable from the solution of Eqs. (6)–(8), of course.

A clear advantage of such an approach is that it provides a quick and easy way of studying phase separation in solid binary alloys for deep quenches, where statistical fluctuations in the final state are not important. This is a quicker alternative to Monte Carlo simulation [44]. While the nearest-neighbor Ising model of a binary alloy is not yet a realistic model of actual alloys, the generalization to include interactions with further neighbors, etc., would be fairly straightforward and, in principle, it should also be possible to use effective interactions derived from electronic structure calculations in this context. Note that many alloys for which spinodal decomposition is experimentally studied [1–6] exhibit complex phase diagrams, where phase separation and superstructure formation may compete. The lattice mean field approach that we propose in this paper should be able to cope with such extensions. Also an extension to a more realistic description of diffusion via vacancies rather than direct *A*-*B* interchanges [41] is conceivable.

The purpose of the present work is to show that indeed such a lattice mean field approach to spinodal decomposition in thin films (and in the bulk) is both feasible and efficient. In Sec. II, we present the discrete lattice analog of Eqs. (1)–(3) and (6)–(8), following up on the work by Binder and Frisch [20]. In Sec. III, we present various numerical results for deep quenches (i.e., temperatures far below criticality) and discuss the resulting structure formation for a symmetric film, both in directions parallel and perpendicular to the walls. In Sec. IV, we present a comparison to the continuum approach, Eqs. (6)–(8). Finally, Sec. V summarizes our paper, containing also an outlook on simulations where the basic atomistic model is not a lattice model, as is the case for spinodal decomposition in fluid binary mixtures.

II. MOLECULAR FIELD THEORY FOR THE KAWASAKI KINETIC ISING MODEL IN A THIN FILM

The system that is considered is the ferromagnetic Ising model with nearest-neighbor exchange on the simple cubic lattice, described by the Hamiltonian

$$\mathcal{H} = -J \sum_{\substack{\langle i,j \rangle \\ \text{bulk}}} S_i S_j - J_s \sum_{\substack{\langle i,j \rangle \\ \mathcal{S}1, \mathcal{S}2}} S_i S_j - H \sum_i S_i - H_{\mathcal{S}1} \sum_{i \in \mathcal{S}1} S_i$$

$$- H_{\mathcal{S}2} \sum_{i \in \mathcal{S}2} S_i. \tag{9}$$

Here $S_i = \pm 1$, lattice sites are labeled by the index i, and the first sum runs over all nearest neighbor pairs except those in the surfaces $\mathcal{S}1$ and $\mathcal{S}2$. Note that now for a film of thickness D, the surfaces $\mathcal{S}1$ and $\mathcal{S}2$ are located at $n=1$ and $n=n_{max} = D+1$, n being an index labeling the lattice planes in the z direction perpendicular to the surfaces. Also note that all distances will be measured in units of the lattice constant a. The term $-H \sum_i S_i$ describes the Zeeman energy, H being the bulk magnetic field, and the sum runs over all sites of the lattice. It should be remembered that in the interpretation of the Ising model related to binary mixtures, spin up corresponding to A and spin down to B, H would correspond to a chemical potential difference between the species.

The molecular field equations for the local magnetization $m_n(\vec{\rho}) = \langle S_i \rangle$ (we denote the index i of a lattice site by the index n of the plane to which it belongs and a coordinate $\vec{\rho}$ in this plane) become [20]

$$m_n(\vec{\rho}) = \tanh \frac{J}{k_B T} \left[m_{n+1}(\vec{\rho}) + m_{n-1}(\vec{\rho}) + \sum_{\Delta\vec{\rho}} m_n(\vec{\rho} + \Delta\vec{\rho}) + \frac{H}{J} \right], \quad 2 \le n \le D, \tag{10}$$

$$m_1(\vec{\rho}) = \tanh \frac{J}{k_B T} \left[m_2(\vec{\rho}) + \frac{J_S}{J} \sum_{\Delta\vec{\rho}} m_1(\vec{\rho} + \Delta\vec{\rho}) + \frac{H_{\mathcal{S}1} + H}{J} \right], \quad n = 1, \tag{11}$$

$$m_{D+1}(\vec{\rho}) = \tanh \frac{J}{k_B T} \left[m_D(\vec{\rho}) + \frac{J_S}{J} \sum_{\Delta\vec{\rho}} m_{D+1}(\vec{\rho} + \Delta\vec{\rho}) + \frac{H_{\mathcal{S}2} + H}{J} \right], \quad n = D+1. \tag{12}$$

Here $\Delta\vec{\rho}$ is a vector connecting site i with one of its four nearest neighbors in a layer. In the bulk, Eq. (10) reduces to the well-known transcendental equation

$$m_b = \tanh \left[\frac{J}{k_B T} (6 m_b + H/J) \right], \tag{13}$$

from which $T_{cb} = 6J/k_B$ straightforwardly follows.

We also note that Eqs. (10)–(12) correspond to the free energy

$$F = \sum_{n=1}^{D+1} (E_n - T S_n) \tag{14}$$

with

$$\frac{S_n}{k_B T} = \sum_{\vec{\rho}} \left\{ \left(\frac{1 + m_n(\vec{\rho})}{2} \right) \ln \left(\frac{1 + m_n(\vec{\rho})}{2} \right) \right.$$
$$\left. + \frac{1 - m_n(\vec{\rho})}{2} \ln \left(\frac{1 - m_n(\vec{\rho})}{2} \right) \right\}, \quad (15)$$

$$E_n = -\sum_{\vec{\rho}} \left\{ m_n(\vec{\rho}) H + \frac{J}{2} m_n(\vec{\rho}) [m_{n-1}(\vec{\rho}) + m_{n+1}(\vec{\rho})] \right.$$
$$\left. + \frac{1}{2} J m_n(\vec{\rho}) \sum_{\Delta\vec{\rho}} m_n(\vec{\rho} + \Delta\vec{\rho}) \right\}, \quad 2 \leq n \leq D, \quad (16)$$

$$E_1 = -\sum_{\vec{\rho}} \left\{ m_1(\vec{\rho})(H + H_1) + \frac{1}{2} J m_1(\vec{\rho}) m_2(\vec{\rho}) \right.$$
$$\left. + \frac{1}{2} J_S m_1(\vec{\rho}) \sum_{\Delta\vec{\rho}} m_1(\vec{\rho} + \Delta\vec{\rho}) \right\}, \quad n = 1, \quad (17)$$

$$E_{D+1} = -\sum_{\vec{\rho}} \left\{ m_{D+1}(\vec{\rho})(H + H_{S2}) + \frac{J}{2} m_{D+1}(\vec{\rho}) m_D(\vec{\rho}) \right.$$
$$\left. + \frac{J_S}{2} m_{D+1}(\vec{\rho}) \sum_{\Delta\vec{\rho}} (\vec{\rho} + \Delta\vec{\rho}) \right\}, \quad n = D + 1. \quad (18)$$

Of course, Eqs. (10)–(12) can be derived from Eq. (14) via

$$\left(\frac{\partial F}{\partial m_n(\vec{\rho})} \right)_{T, H, H_1, \{m_n(\vec{\rho})\}'} = 0. \quad (19)$$

The prime on $\{m_n(\vec{\rho})\}'$ indicates that all local magnetizations are held constant except the one that appears in the considered derivative. Of course, in equilibrium there is no explicit dependence on $\vec{\rho}$, although there clearly is a dependence on n.

However, already in equilibrium the $\vec{\rho}$ dependence is useful, when it is understood that the bulk field has a $\vec{\rho}$ depen-

dence. Considering a wave-vector-dependent bulk field, one then can derive from Eq. (10) for $D \to \infty$ the wave-vector-dependent susceptibility $\chi(\vec{k})$. By linear response to the wave-vector-dependent field one finds, as is well known,

$$\chi(\vec{k}) = \frac{1}{k_B T} \frac{1 - m_b^2}{1 - [J(\vec{k})/k_B T](1 - m_b^2)}, \quad (20)$$

where $J(\vec{k})$ is the Fourier transform of the exchange interaction, i.e., in our case

$$J(\vec{k}) = 2J[\cos(k_x a) + \cos(k_y a) + \cos(k_z a)] \simeq 6J - Jk^2 a^2. \quad (21)$$

From Eqs. (20) and (21) we readily see that

$$\chi(\vec{k}) = \chi(0)/[1 + k^2 \xi^2 a^2], \quad \chi(0) = 1 / \left[\frac{k_B T}{1 - m_b^2} - k_B T_{\text{cb}} \right] \quad (22)$$

and

$$\xi^2 = \frac{J}{\dfrac{k_B T}{1 - m_b^2} - k_B T_{\text{cb}}}. \quad (23)$$

Equation (23) reduces to the result quoted in Eq. (5) when $T \to T_{\text{cb}}$, but also shows that $\xi \to 0$ when $T \to 0$.

As discussed in Ref. [20], we associate dynamics to the Ising model via the Kawasaki spin exchange model [41], considering exchanges between nearest neighbors only. Following the method of Ref. [40], one obtains with the help of the Glauber [45] transition probability a set of coupled kinetic equations for the local time-dependent mean magnetizations $\langle S_i(t) \rangle \equiv m_n(\vec{\rho}, t)$ from the (exact) master equation [41] in molecular field approximation. Denoting the time scale in the transition probability as τ_S, this set of equations is

(i) $3 \leq n \leq D - 1$ (bulk case)

$$2\tau_S \frac{d}{dt} m_n(\vec{\rho}, t) = -6m_n(\vec{\rho}, t) + m_{n-1}(\vec{\rho}, t) + m_{n+1}(\vec{\rho}, t) + \sum_{\Delta\vec{\rho}} m_n(\vec{\rho} + \Delta\vec{\rho}, t) + [1 - m_n(\vec{\rho}, t) m_{n-1}(\vec{\rho}, t)]$$

$$\times \tanh \frac{J}{k_B T} \left[m_{n+1}(\vec{\rho}, t) + m_{n-1}(\vec{\rho}, t) + \sum_{\Delta\vec{\rho}} m_n(\vec{\rho} + \Delta\vec{\rho}, t) - m_n(\vec{\rho}, t) - m_{n-2}(\vec{\rho}, t) - \sum_{\Delta\vec{\rho}} m_{n-1}(\vec{\rho} + \Delta\vec{\rho}, t) \right]$$

$$+ [1 - m_n(\vec{\rho}, t) m_{n+1}(\vec{\rho}, t)] \tanh \frac{J}{k_B T} \left[m_{n+1}(\vec{\rho}, t) + m_{n-1}(\vec{\rho}, t) + \sum_{\Delta\vec{\rho}} m_n(\vec{\rho} + \Delta\vec{\rho}, t) - m_n(\vec{\rho}, t) - m_{n+2}(\vec{\rho}, t) \right.$$

$$\left. - \sum_{\Delta\vec{\rho}} m_{n+1}(\vec{\rho} + \Delta\vec{\rho}, t) \right] + \sum_{\Delta\vec{\rho}} [1 - m_n(\vec{\rho}, t) m_n(\vec{\rho} + \Delta\vec{\rho}, t)] \tanh \frac{J}{k_B T} \left[m_{n+1}(\vec{\rho}, t) + m_{n-1}(\vec{\rho}, t) + \sum_{\Delta\vec{\rho}'} m_n(\vec{\rho} + \Delta\vec{\rho}', t) \right.$$

$$\left. - m_{n+1}(\vec{\rho} + \Delta\vec{\rho}, t) - m_{n-1}(\vec{\rho} + \Delta\vec{\rho}, t) - \sum_{\Delta\vec{\rho}'} m_n(\vec{\rho} + \Delta\vec{\rho} + \Delta\vec{\rho}', t) \right]. \quad (24)$$

Factors such as $[1 - m_n m_{n-1}]$ arise from the mean-field approximations to factors $(1 - S_i S_j)$ that express the fact that an exchange of S_i with S_j changes the magnetization S_i only if S_i and S_j are oppositely oriented. In Eq. (24), exchanges of a spin

at site $\vec{\rho}$ in layer n with spins in layers $n-1$, $n+1$, and the same layer n need to be considered. In the argument of the tanh functions, the difference of the effective fields acting on the spins that are exchanged is found. One can verify that Eq. (24) reduces to Eq. (10) if $dm_n(\vec{\rho},t)/dt=0$ is assumed: in equilibrium, the exchange of a spin with another one is exactly compensated by the inverse process. The kinetic equations near the wall are similar; one has to consider that in layer 1 a field $H_{\mathcal{S}1}$ is acting, and that no spin exchange into the layer $n=0$ (the wall) is possible. Hence, for (ii) $n=2$

$$2\tau_S\frac{d}{dt}m_2(\vec{\rho},t) = -6m_2(\vec{\rho},t) + m_1(\vec{\rho},t) + m_3(\vec{\rho},t) + \sum_{\Delta\vec{\rho}}m_2(\vec{\rho}+\Delta\vec{\rho},t)$$

$$+[1-m_2(\vec{\rho},t)m_1(\vec{\rho},t)]\tanh\frac{J}{k_BT}\left[m_3(\vec{\rho},t)+m_1(\vec{\rho},t)+\sum_{\Delta\vec{\rho}}m_2(\vec{\rho}+\Delta\vec{\rho},t)-\frac{H_{\mathcal{S}1}}{J}-m_2(\vec{\rho},t)-\frac{J_S}{J}\sum_{\Delta\vec{\rho}}m_1(\vec{\rho}+\Delta\vec{\rho},t)\right]$$

$$+[1-m_2(\vec{\rho},t)m_3(\vec{\rho},t)]\tanh\frac{J}{k_BT}\left[m_3(\vec{\rho},t)+m_1(\vec{\rho},t)+\sum_{\Delta\vec{\rho}}m_2(\vec{\rho}+\Delta\vec{\rho},t)-m_4(\vec{\rho},t)-m_2(\vec{\rho},t)-\sum_{\Delta\vec{\rho}}m_3(\vec{\rho}+\Delta\vec{\rho},t)\right]$$

$$+\sum_{\Delta\vec{\rho}}[1-m_2(\vec{\rho},t)m_2(\vec{\rho}+\Delta\vec{\rho},t)]\tanh\frac{J}{k_BT}\left[m_3(\vec{\rho},t)+m_1(\vec{\rho},t)+\sum_{\Delta\vec{\rho}}m_2(\vec{\rho}+\Delta\vec{\rho},t)\right]$$

$$-m_3(\vec{\rho}+\Delta\vec{\rho},t)-m_1(\vec{\rho}+\Delta\vec{\rho},t)-\sum_{\Delta\vec{\rho}'}m_2(\vec{\rho}+\Delta\vec{\rho}+\Delta\vec{\rho}',t) \tag{25}$$

and for (now only five neighbors are available for an exchange) (iii) $n=1$

$$2\tau_S\frac{d}{dt}m_1(\vec{\rho},t)=-5m_1(\vec{\rho},t)+m_2(\vec{\rho},t)+\sum_{\Delta\vec{\rho}}m_1(\vec{\rho}+\Delta\vec{\rho},t)+[1-m_1(\vec{\rho},t)m_2(\vec{\rho},t)]\tanh\frac{J}{k_BT}$$

$$\times\left[m_2(\vec{\rho},t)+\frac{H_{\mathcal{S}1}}{J}+\frac{J_S}{J}\sum_{\Delta\vec{\rho}}m_1(\vec{\rho}+\Delta\vec{\rho},t)-m_3(\vec{\rho},t)-m_1(\vec{\rho},t)-\sum_{\Delta\vec{\rho}}m_2(\vec{\rho}+\Delta\vec{\rho},t)\right]+\sum_{\Delta\vec{\rho}}[1-m_1(\vec{\rho},t)m_1(\vec{\rho}+\Delta\vec{\rho},t)]$$

$$\times\tanh\frac{J}{k_BT}\left[m_2(\vec{\rho},t)+\frac{J_S}{J}\sum_{\Delta\vec{\rho}'}m_1(\vec{\rho}+\Delta\vec{\rho}',t)-m_2(\vec{\rho}+\Delta\vec{\rho},t)-\frac{J_S}{J}\sum_{\Delta\vec{\rho}'}m_1(\vec{\rho}+\Delta\vec{\rho}'+\Delta\vec{\rho},t)\right]. \tag{26}$$

The equations for $n=D$ and $n=D+1$ are analogous. The time t in Eqs. (24)–(26) is related to time τ in Eqs. (6)–(8) via

$$\tau=\frac{T_{cb}/T-1}{8\tau_s\xi^2}. \tag{27}$$

In Ref. [20], equations closely related to Eqs. (24)–(26) were already written down for a semi-infinite system instead of a thin film geometry but no numerical solution was attempted, rather these equations were linearized (which is useful for temperatures above criticality and weak enough surface fields) to enable an analytic solution. This work hence could only deal with (weak) surface enrichment in the disordered phase of the alloy, not at all with spinodal decomposition. In addition, Ref. [20] used these equations to derive boundary conditions for the continuum limit, which later were replaced [8] by Eqs. (7) and (8). Thus, the possibility of solving Eqs. (24)–(26) as they stand has not been considered before. The numerical solutions of the set of equations (24)–(26) for quenching experiments from infinite temperature to the states inside the miscibility gap is the subject of the next section.

III. NUMERICAL RESULTS FOR PHASE SEPARATION FOLLOWING DEEP QUENCHES

In this section we shall present selected results from the numerical solutions of Eqs. (24)–(26), choosing three values

of the thickness of the film ($D=9$, 19, and 29, corresponding to $n_{max}=10$, 20, and 30 lattice planes, respectively), and a quench at time $t=0$ from infinite temperature to $T/T_{cb}=2/3$, for the special cases $H_{\mathcal{S}1}=H_{\mathcal{S}2}=1.0$, 0.1, and $J_S=J$. The initial conditions for $m_n(\vec{\rho},t)$ is chosen by taking $m_n(\vec{\rho},0)$ from a random uniform distribution between -1 and $+1$, with the total magnetization in the thin film zero.

At first sight a quench to $T/T_{cb}=2/3$ does not look to be a particularly deep quench. However, one must keep in mind that in order to have ξ larger (or equal) than a lattice spacing one must have $T\gtrsim5.57J/k_B$, i.e., much closer to $T_{cb}=6J/k_B$. At the present temperature $k_BT/J=4.0$, the correlation length is as small as $\xi\simeq0.33$ lattice spacings. Following the standard reasoning for the simulation of the Ginzburg-Landau model, Eqs. (6)–(8), one should choose 2ξ as the size of the spatial discretization mesh: dealing with the above physical film thickness would require rather huge lattices. In addition, Eqs. (1)–(3) do not represent the actual free energies of the lattice model [Eqs. (14)–(18)] accurately at such low temperatures either.

Choosing the time unit $\tau_s=1$ in Eqs. (24)–(26) we have found that accurate numerical solutions of these equations result already when one chooses a rather large discrete time step $\delta t=0.1$. Other than this discretization of time no approximations whatsoever enter the numerical solution. Of
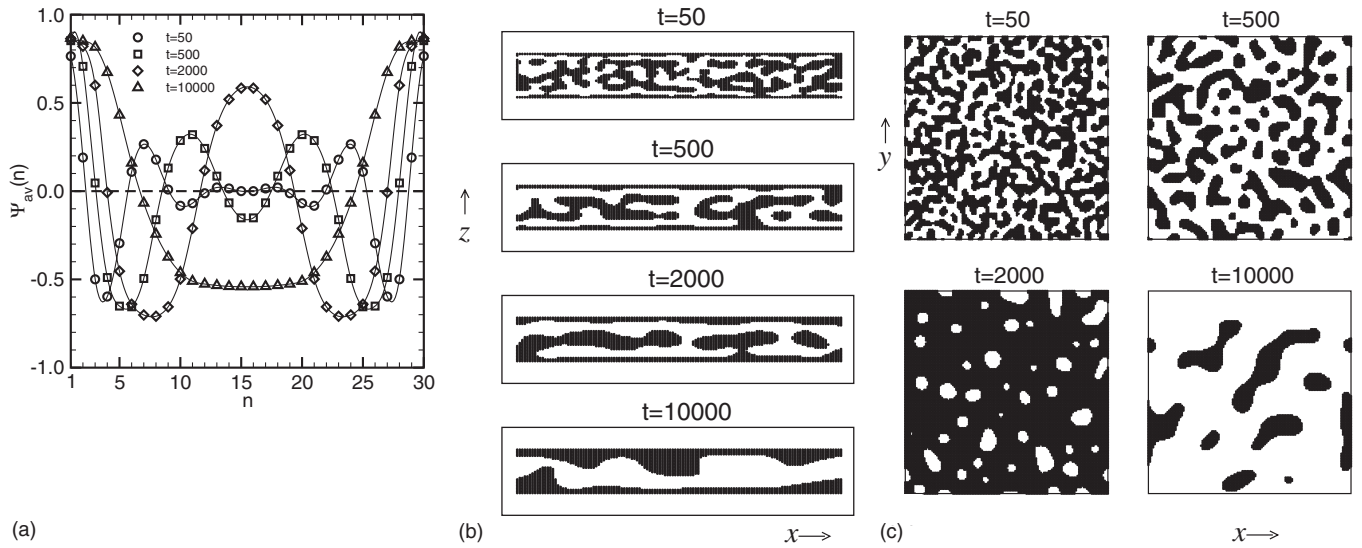
FIG. 1. (a) Layerwise order parameter $\Psi_{av}(n)$ plotted vs layer index n for four different times for the choice $D=29$, $L=128$, $k_BT=4J$, and $H_{S1}=H_{S2}=1.0$. The continuous lines are cubic interpolations to the original data, used as guides to the eye. (b) Cross-sectional snapshot pictures of the same systems as in (a), displaying the magnetization configuration in the xz plane for $y=L/2$. If the magnetization at a lattice site is positive, a black dot is printed. (c) Same as (b), but for a plane parallel to the walls, at $n=15$.

course, one always has to deal with a finite system geometry also in lateral directions: unless otherwise mentioned we choose $L_x=L_y=L=128$ for all values of D and apply periodic boundary conditions in both directions.

Figure 1 shows data for a typical time evolution for $D=29$ and $H_{S1}=H_{S2}=1.0$. In Fig. 1(a), we show the layerwise average order parameter $\Psi_{av}(n)=L^{-2}\Sigma_{\vec{\rho}}m_n(\vec{\rho},t)$ as a function of the layer index n. One sees that in the surface planes the magnetization takes its saturation value rather fast, as expected due to the large surface fields. Then the magnetization decreases very rapidly, already for $n=3$ the magnetization for $t=50$ is strongly negative. For $t=50$ the curve $\Psi_{av}(n)$ then exhibits the oscillations typical for "surface-directed spinodal decomposition" [7–19], with a second maximum at $n=7$ and a (weak) third one at $n=13$. Because of the symmetric surface fields, it is expected that the profile should be symmetric around the center of the film

$$\Psi_{av}(n) = \Psi_{av}(D-n+2). \qquad (28)$$

But in reality this is not obeyed because of finite system size and lack of averaging over sufficiently large number of independent initial configurations (in our case averaging was done only over five independent random initial configurations). However, all plots for $\Psi_{av}(n)$ have been symmetrized by hand by taking advantage of property (28).

One can further see from Fig. 1(a) that the thickness of the surface enrichment layers at the walls slowly grows with increasing time, which is also obvious from Fig. 1(b) where we present the snapshot pictures of vertical sections (xz plane). At a later time the position of the second peak of $\Psi_{av}(n)$ has moved towards the center (it now occurs at $n=11$ for $t=500$) with a pronounced minimum in the center of the film. However, for $t\geq 2000$ this second peak has merged with its mirror image, i.e., now in the film center
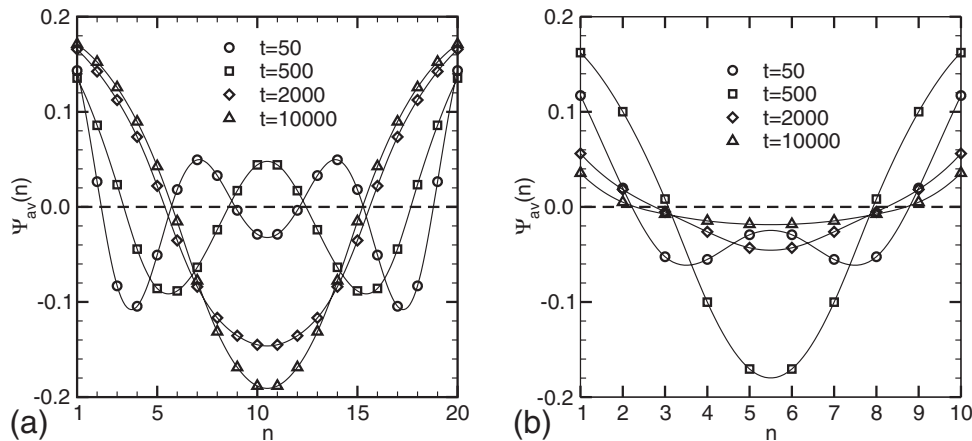

FIG. 2. Layerwise average order parameter $\Psi_{av}(n)$ plotted vs n for four different times for the cases (a) $D=19$, $L=128$ and (b) $D=9$, $L=128$. Always $H_{S1}=H_{S2}=0.1$ and $k_BT=4J$ are chosen.
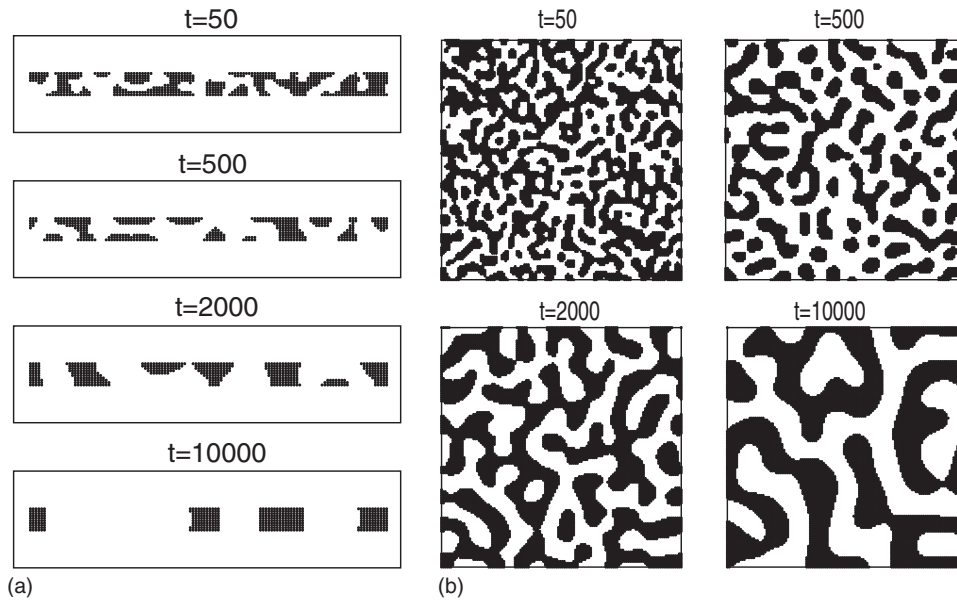
FIG. 3. Cross-sectional snapshot pictures of the system with $D=9$, $L=128$, $H_{S1}=H_{S2}=0.1$ for (a) the xz plane and (b) the xy plane at $n=5$ for the same system as in Fig. 2(b).

there is a maximum of $\Psi_{av}(n)$ rather than a minimum. At very late time, this central maximum has disappeared again ($t=10\,000$) and the profile looks like that of a simple stratified structure. Actually this is not the case, as seen in Fig. 1(c), where we have shown the snapshot pictures parallel to the surfaces (xy plane) for $n=15$. As is also observed in the Ginzburg-Landau studies of surface-directed spinodal decomposition [8–10,12–14,17,18], in the lateral directions one can observe initially a rather random pattern which rapidly coarsens with increasing time.

Figure 2 shows other examples where we have chosen thinner films (viz., $D=9$ and $D=19$) and a much weaker boundary field ($H_{S1}=H_{S2}=0.1$). Now the amplitude of the variation of $\Psi_{av}(n)$ is much smaller, and at late times the order parameter profiles across the film have almost no structure. The explanation for this behavior is seen in Fig. 3 where we show snapshot pictures of the states evolving for

the choice $D=9$ of Fig. 2(b): The system develops towards a two-dimensional arrangement of columns of positive magnetization connecting the two walls, and thus in each plane ($n=\text{const}$), there is only a weak excess of magnetization in any one direction. These results qualitatively do not differ from the numerical studies of spinodal decomposition in thin films based on the Ginzburg-Landau (GL) equation, such as Ref. [18]; however, the advantage of the present treatment is that the parameters of the model have an immediate and straightforward physical meaning. The fact that in the late stages there is almost no nontrivial structure across the film is also evident from a comparison of the pair correlation function $C_n(\rho,t)$ $[=\langle m_n(\vec{0},t)m_n(\vec{\rho},t)\rangle - \langle m_n(\vec{0},t)\rangle\langle m_n(\vec{\rho},t)\rangle]$ and their Fourier transforms $S_n(k,t)$ in different layers, shown in Fig. 4.

In Fig. 5(a), the plot of the time evolution of $C_n(\rho,t)$, for $n=5$, for the same system as in Fig. 3, clearly reflects the
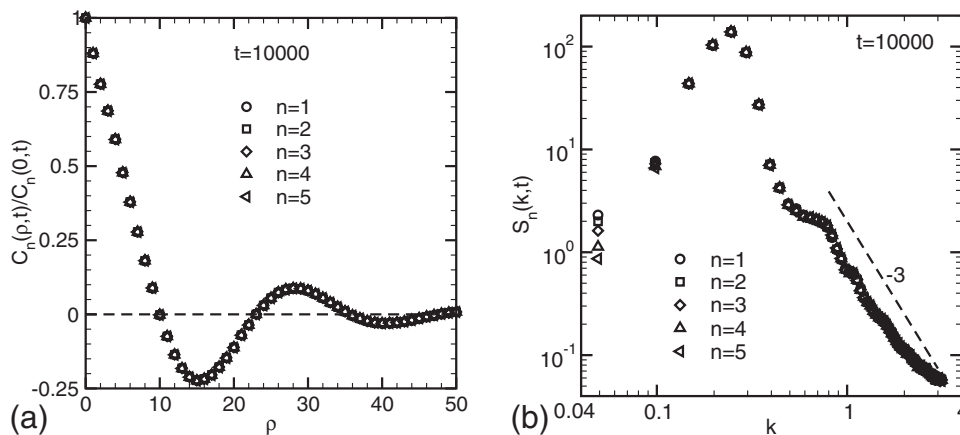

FIG. 4. (a) Layerwise correlation function $C_n(\rho,t)$ plotted vs ρ, for the choice $H_{S1}=H_{S2}=0.1$, $k_BT=4J$, $D=9$, $L=128$, $t=10\,000$. Data for $n=1, 2, 3, 4,$ and 5 superimpose almost exactly. (b) Fourier transform $S_n(k,t)$ of $C_n(\rho,t)$, again resolved with respect to individual layers. In (b) the dashed line corresponds to the Porod tail k^{-3}.
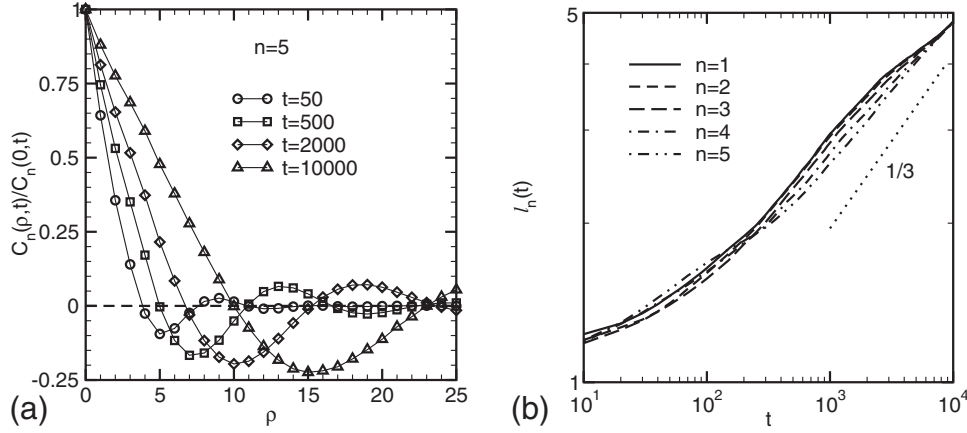
FIG. 5. (a) Same as Fig. 4(a) but only for $n=5$, and four times as indicated. (b) Characteristic domain length $l_n(t)$ of individual layers, shown on a log-log plot versus time t. The dotted line corresponds to LS growth law $t^{1/3}$.

coarsening behavior. Note that the apparent nonscaling behavior of $C_n(\rho,t)$ is due to strong fluctuation of the layerwise average order parameter at early time. In Fig. 5(b) we plot the layerwise average domain size $l_n(t)$ as a function of t extracted from the condition $C_n[\rho=l_n(t),t]=C_n(0,t)/2$. The characteristic length $l_n(t)$ initially grows rather slowly, for times $10 < t < 1000$ there is considerable curvature on the log-log plot, while for $t \gtrsim 1000$ the behavior is already close to the standard Lifshitz-Slyozov (LS) [46] $l(t) \propto t^{1/3}$ law. The fact that the "effective exponent" $d[\ln l(t)]/d(\ln t)$ approaches $1/3$ from below is quite reminiscent of Monte Carlo simulations of coarsening in the two-dimensional Kawasaki spin-exchange model [44], of course. It should be noted that Monte Carlo simulations include thermal fluctuations that are absent in our molecular field treatment. However, it is generally believed [4] that thermal fluctuations are irrelevant during the late stages of coarsening. In view of these facts, the similarity of our results with the previous Monte Carlo studies of coarsening on lattice models is not unexpected. The advantage of the present approach in comparison with Monte Carlo, however, is that much less numerical effort is needed.

IV. THE CRITICAL REGION: A COMPARISON BETWEEN THE LATTICE APPROACH AND THE GINZBURG-LANDAU TREATMENT

Near the critical point one must take into account that the critical point is slightly shifted to lower temperatures for films of finite thickness as compared to the bulk [21,31–34]. In Fig. 6(a), we plot the critical temperatures $T_c(D)$ for films of finite width as a function of width D. The numerical values for $T_c(D)$ were obtained by solving Eqs. (10)–(12) for $H=H_{S1}=H_{S2}=0$ starting with the assignment of uniform magnetization to the layers in a random fashion so that the total film magnetization is zero. Note that as $D \to \infty$, $T_c(D)$ is expected to approach its three-dimensional (3D) mean field value $6J/k_B=T_{cb}$ and in the limit $D \to 0$, we expect the 2D value $4J/k_B$. In Fig. 6(b), we present the deviation of $T_c(D)$ from T_{cb} as a function of D on a log-log plot. From finite-size scaling theory, this difference should vanish as $T_{cb}-T_c(D) \sim D^{-2}$.

While for $D=29$ we have $T_c(D) \simeq 5.99J/k_B$, for $D=9$ we have $T_c(D) \simeq 5.92J/k_B$. Since lateral phase separation occurs only for $T < T_c(D)$ [35–37], of course, this shift restricts the
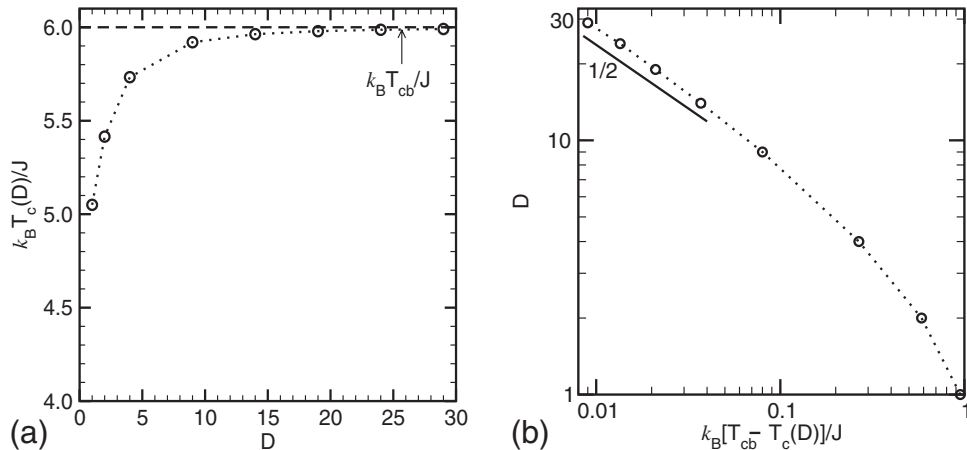

FIG. 6. Plot of finite-size critical temperature $T_c(D)$ versus film thickness D, (a) on a linear scale and (b) on a log-log plot to display the asymptotic behavior $T_{cb}-T_c(D) \propto D^{-2}$ of mean-field theory. The dashed line in (a) marks the bulk critical temperature, whereas the continuous line in (b) corresponds to the asymptotic theoretical prediction.
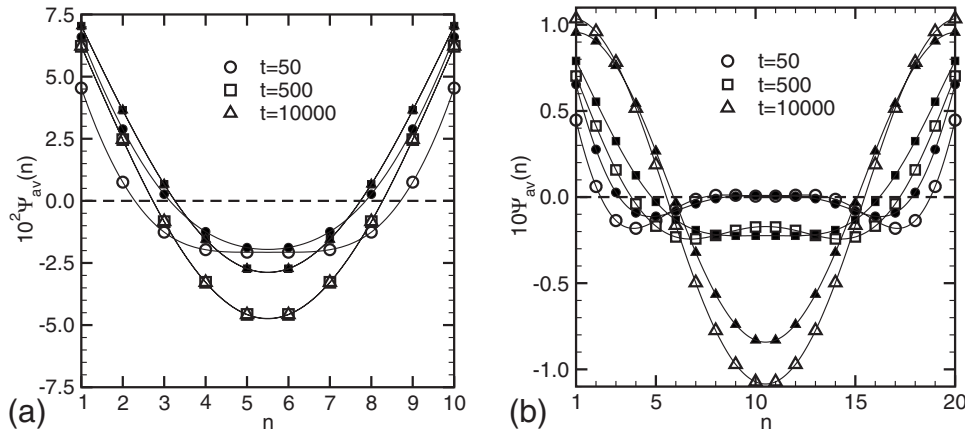
FIG. 7. Comparison of the layerwise average order parameter profiles across the film for three times ($t=50$, 500, and 10 000, respectively), according to the lattice model (open symbols) and the GL model (filled symbols), for (a) $D=9$ and (b) $D=19$, respectively. All data refer to the choice $H_{S1}=H_{S2}=0.1, k_B T/J=5.875$.

range of ξ that can be studied for the present choices of D. While $2\xi \simeq 1.0$ occurs for $T=4.75J/k_B$ and hence this choice, for which the cell size of the Ginzburg Landau model agrees with the lattice spacing of the molecular field model, is safely accessible, already for $\xi \simeq 2.0$ (occurring for $k_B T = 5.875J$) we are only slightly below $T_c(D=9)$, and for $\xi = 3$ we would already be in the one-phase region of such a thin film. In view of these considerations, $k_B T = 5.875J$ was chosen as a temperature where it makes sense to compare the lattice model with $D=9$, 19, and 29 (i.e., $n_{max}=10$, 20, and 30 lattice planes, respectively) with the corresponding GL model. Note that for the convenience of comparison as well as accuracy of numerical solutions, the discrete mesh sizes Δx, Δy, and Δz in the GL model were adjusted to the lattice constant a and we have set $\tau_0 = 0$.

In Fig. 7 we present the comparison between the lattice model and GL model at $k_B T = 5.875J$ ($\xi \simeq 2.0$, $m_b \simeq 0.25$) with $H_{S1}=H_{S2}=0.1$ for $D=9$ and 19. At this temperature the parameters h_{S1}, g, γ, τ have the values 52.3 ($523H_{S1}$), -128, 32, and $t/1600$, respectively. One sees that for $D=9$ [Fig. 7(a)] the behavior of the lattice model and the GL model are qualitatively similar, but there is no quantitative agreement. These discrepancies do get smaller, however, with increasing

film thickness [Fig. 7(b)]. In Fig. 8, where we plot the order parameter profile for $D=29$ corresponding to two values of surface fields (see caption for details), we see that the discrepancies between the lattice and GL models are already quite small, irrespective of the choice of the surface field. However, for stronger surface field [Fig. 8(b)], the discrepancy is still visible at the surfaces. Presumably the discrepancy for small film thicknesses could be reduced by following the approach of Fukuda *et al.* [43] using a mesh that is finer than the lattice spacing and hence avoid problems with nonconserved evolution equations for the order parameter at the surface. These problems still are nonnegligible if the correlation length is only twice as large as the lattice spacing. As mentioned above, Eqs. (29) and (30) become strictly correct only in the limit where the correlation length becomes infinite (i.e., asymptotically close to the critical point in a semi-infinite system). In the immediate vicinity of the critical point, the close correspondence between the time evolution predicted by the lattice theory and the GL model is also evident when one compares snapshot pictures of the time evolution, shown in Figs. 9 and 10, generated at $k_B T/J = 5.875$ corresponding to $H_{S1}=H_{S2}=0.1$, $D=29$, for both the models. However these snapshots suggest that at this tem-
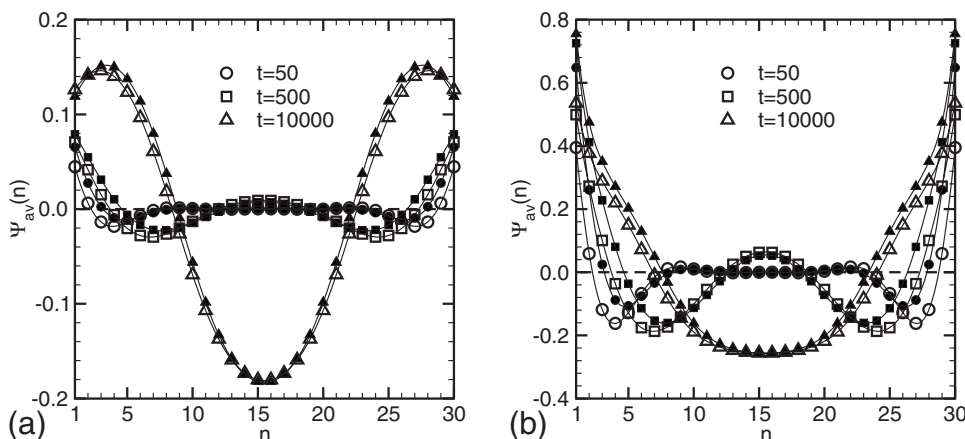

FIG. 8. Same as Fig. 7, but for $D=29$, and two choices of the strength of the surface fields $H_{S1}=H_{S2}=0.1$ (a) and 1.0 (b).
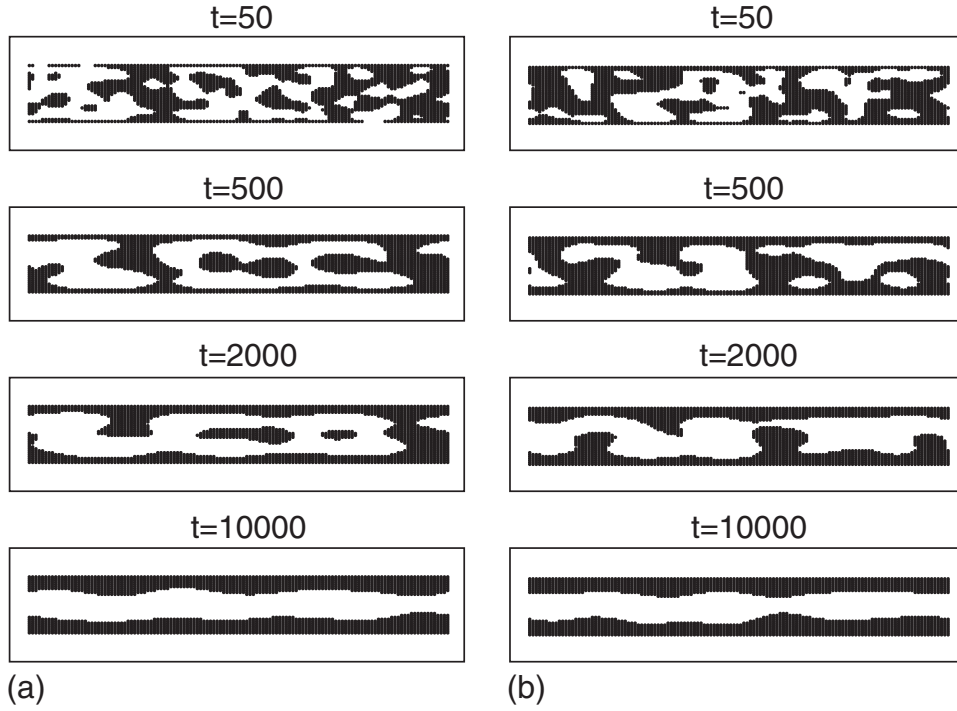
FIG. 9. Cross-sectional snapshot pictures in the xz plane, for $D=29$, $H_{S1}=H_{S2}=0.1$, at $k_BT/J=5.875$ [same system as in Fig. 8(a)], for four different times as indicated, according to (a) the lattice model and (b) the Ginzburg-Landau model.

perature the lateral inhomogeneity disappears in the late stages of the phase separation process. Note that due to the proximity of the critical point, which for finite D is shifted and nonzero surface fields, the coexistence curve separating the two-phase region from the one-phase region may be considerably distorted [29,31]. In view of that, it is plausible that the state point for small D falls in the one-phase region of the thin film. However, this did not happen in the present case, as is clear from Fig. 11, where we have shown snapshot pictures over a much longer time scale for a system with all parameters same as in Figs. 9 and 10 except now we have $D=19$, $L=64$. So, the apparent stratified structure in Figs. 9 and 10 is temporary which disappears at a later time.

In Fig. 12 we show comparisons at lower temperatures, viz., $k_BT=5.57J$ ($\xi \simeq 1.0$, $m_b \simeq 0.45$, $h_{S1} \simeq 15.4H_{S1}$, $g=-8$, $\gamma=4$, $\tau \simeq t/104$) and $k_BT \simeq 4.75J$ ($\xi \simeq 0.5$, $m_b \simeq 0.72$, $h_{S1} \simeq 0.44H_{S1}$, $g=-0.5$, $\gamma=0.5$, $\tau \simeq t/7.6$). For both the temperatures we have set $H_{S1}=H_{S2}=0.1$. Rather pronounced discrepancies between the lattice model and the GL model do occur, however, at low temperature [Fig. 12(b)], as expected.

Note that the prefactor γ [see Eq. (4)] in the scaled Eq. (7) is an approximation which applies in the close vicinity of the critical point [8]. Here we try to take into account correction terms to the leading behavior of Eq. (7) to make the GL model more accurate for temperatures away from criticality. The order parameter $\phi(\vec{\rho},z,t)$ (not normalized by m_b, and
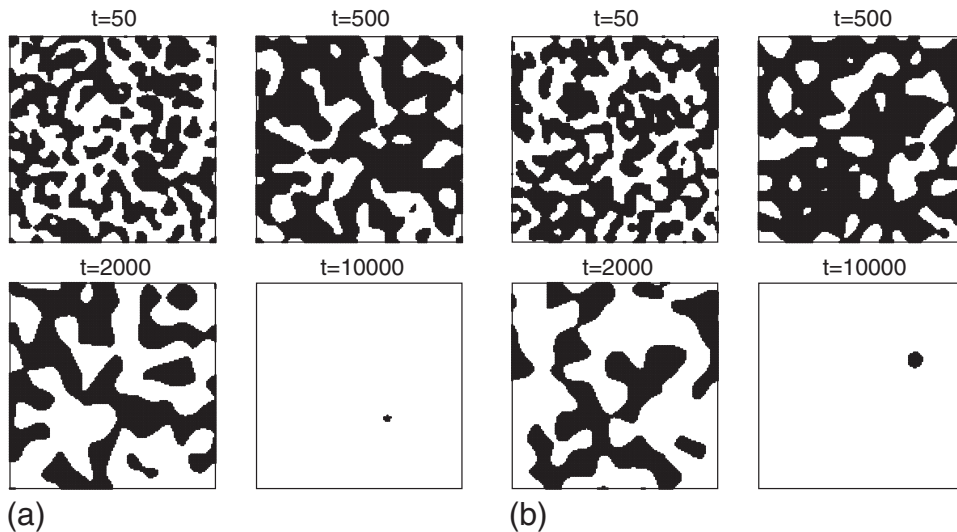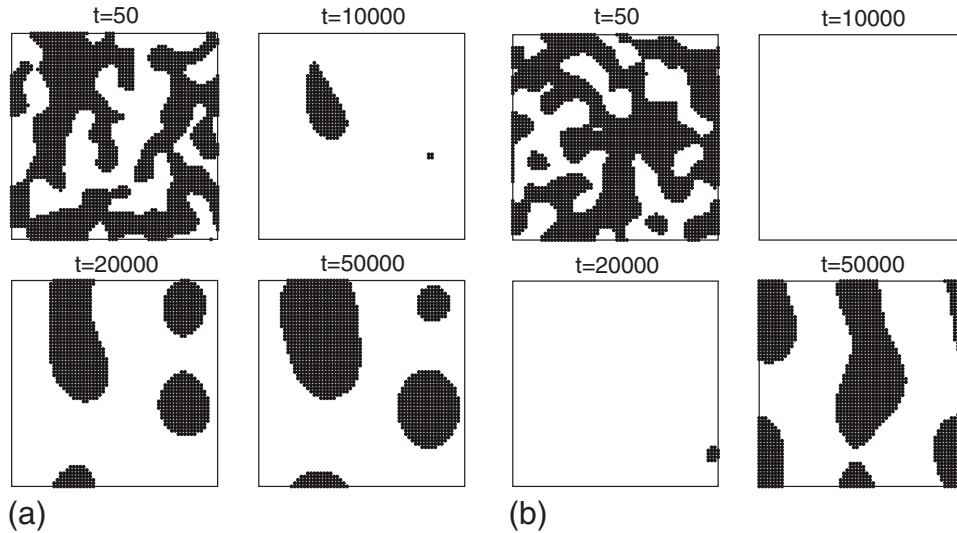

FIG. 10. Same as Fig. 9, but for a plane at $n=15$, parallel to the walls.

FIG. 11. Same as Fig. 10, but for $D=19$, $L=64$, at $n=10$.

lengths not rescaled by 2ξ) satisfies the boundary conditions [8]

$$2\tau_s \frac{\partial \phi(\vec{\rho}, z=0, t)}{\partial t} = \frac{H_1}{T} + \frac{J}{T}\left(4\frac{J_s}{J} - 5\right)\phi(\vec{\rho}, z=0, t)$$
$$- \left(\frac{T_{cb}}{T} - 1 - \frac{J}{T}\right) \left.\frac{\partial \phi(\vec{\rho}, z, t)}{\partial z}\right|_{z=0}, \tag{29}$$

$$\frac{\partial}{\partial z}\left\{\left(\frac{T_{cb}}{T} - 1\right)\phi(\rho, z, t) - \frac{1}{3}[\phi(\rho, z, t)]^3\right.$$
$$\left.+ \frac{J}{T}\frac{\partial^2}{\partial z^2}[\phi(\rho, z, t)]\right\}\Bigg|_{z=0} = 0. \tag{30}$$

From Eq. (29) we see, however, that a pathological behavior occurs if the coefficient $(T_{cb}/T-1-J/T)$ vanishes, which is the case for $k_B T/J = 5$: the time evolution of $\phi(\vec{\rho}, z=0, t)$ then is strictly decoupled from the order param-

eter in the interior, and it stops if $\phi(\vec{\rho}, z=0, t)$ reaches the value H_{S1}/J (for $J_s/J=1$). This is what is seen in Fig. 13(a), where we have solved the unscaled version of the GL model. In this case $\Psi_{av}(z=0, t)$ has stopped its time evolution already during the very early stages. For $k_B T < 5J$ [Fig. 13(b)], the coefficient of the last term on the right side in Eq. (29) has changed its sign (in comparison to the region close to T_{cb}), and this leads to the result that $\phi(\vec{\rho}, z=0, t)$ converges to zero, which also is unreasonable. Thus, taking the coefficient $(T_{cb}/T - 1 - J/T)$ rather than simply $(-J/T)$ [the latter leads to the scaled form Eq. (7) with the coefficient γ as quoted in Eq. (4)] does not yield any improvement, but rather is physically inconsistent. However, working with the scaled form of the GL equations, and their boundary conditions, Eqs. (4)–(8) does not yield results in agreement with the lattice model at temperatures $k_B T/J \lesssim 5$ either.

V. CONCLUSION

In this paper we have presented a molecular field theory for the Kawasaki spin-exchange Ising model in a thin film
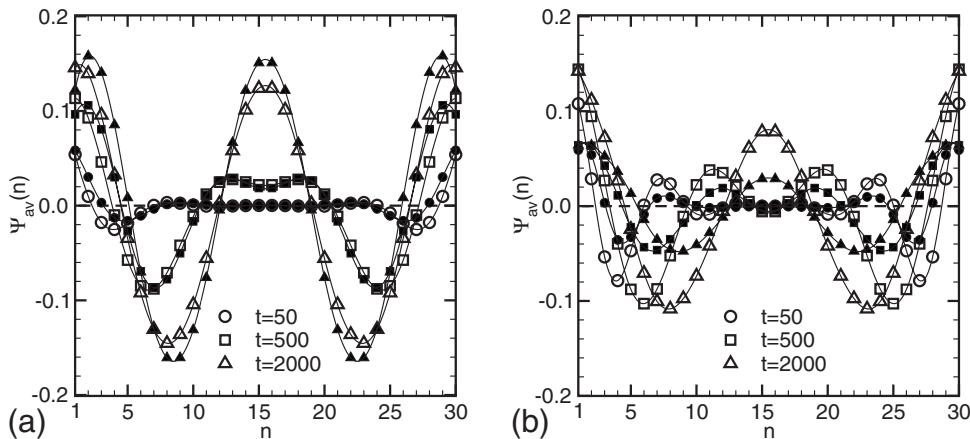

FIG. 12. Plot of $\Psi_{av}(n)$ vs n for $D=29$ with $H_{S1}=H_{S2}=0.1$ at temperatures (a) $k_B T=5.57J$ and (b) $k_B T=4.75J$. The open symbols corresponds to the lattice model whereas the filled symbols are for the GL model. Note that $k_B T=5.57J$ corresponds to bulk correlation length $\xi \simeq 1.0$ and at $k_B T=4.75J$, $\xi \simeq 0.5$.
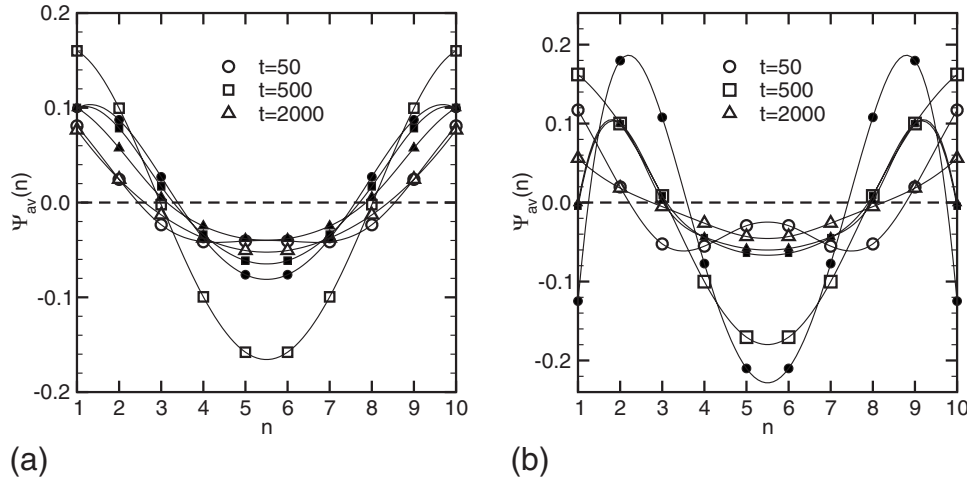
FIG. 13. Comparison between the unscaled GL model [see Eqs. (29) and (30)] and lattice model at temperatures (a) $5J/k_B$ and (b) $4J/k_B$. Note that the open symbols are for lattice model and the filled symbols are used for the unscaled GL model.

geometry and have shown that the numerical solution of the resulting set of coupled ordinary differential equations describing the time dependence of the local magnetization at the lattice sites is a convenient and efficient method to study spinodal decomposition of such systems, taking the boundary conditions at the surfaces of the film properly into account. Obviously, in comparison to a Monte Carlo simulation of this model one has lost thermal statistical fluctuations, except for those built into the theory via the choice of noise in the initial configuration of the system; but there is consensus [1–5] that for a description of the late stage coarsening behavior such thermal fluctuations may safely be neglected. Thus, the present method is favorable in comparison with Monte Carlo, since the code runs much faster.

In the vicinity of the critical point, where the correlation length ξ is sufficiently large, and also the film thickness D is sufficiently large as well, our treatment becomes equivalent to the time-dependent Ginzburg-Landau theory. However, one needs to go surprisingly close to the critical point of the bulk to actually demonstrate this limiting behavior from our lattice model treatment numerically. The GL treatment over most of the parameter regime provides only a qualitative, rather than quantitative, description of the system. In principle, for the GL theory to be accurate, the correlation length should be much larger than the lattice spacing. However, this happens only very close to the critical point. In our nearest-neighbor Ising model on the simple cubic lattice, the approach followed in Refs. [8,10,12–14,17,18] becomes equivalent to the lattice molecular field approach only when the temperature exceeds about 97.9% of the mean field critical temperature ($6J/k_B$) because only then will the correlation length exceed two lattice spacings. However, then thermal fluctuations modify the behavior substantially (e.g., the actual bulk critical temperature is only about $4.51J/K_B$). So

the GL theory of Refs. [8,10,12–14,17,18] should only be considered as a generic qualitative model, but not as a quantitative description of specific systems. Away from the critical points no well-defined connection to the parameters of a microscopic Hamiltonian can be made for the GL theory, while the present lattice approach has this connection by construction.

Of course, the problem of surface-directed spinodal decomposition is most interesting for liquid binary mixtures, for which our lattice model is inappropriate due to the lack of hydrodynamic interactions; even for solid mixtures (two different atomic species sharing the sites of a lattice) our model is an idealization (neither elastic distortions nor lattice defects were included; actual solid binary mixtures decompose via the vacancy mechanism of diffusion [1,2], etc.). While GL models including hydrodynamic interactions have been formulated [1–5], the restriction that any GL model is valid only in the immediate neighborhood of the critical point applies there as well. While outside the critical region unmixing of fluids can be simulated by molecular dynamics methods (see, e.g., Ref. [19]), such simulations are extremely time consuming, and an analog of the present dynamic mean field theory for inhomogeneous fluids would be very desirable. Developing such an approach clearly is a challenge for the future.

[1] K. Binder and P. Fratzl, in *Phase Transformations in Materials*, edited by G. Kostorz (Wiley-VCH, Weinheim, 2001), p. 409.

[2] A. Onuki, *Phase Transition Dynamics* (Cambridge University Press, Cambridge, 2002).

[3] J. D. Gunton, M. San Miguel, and P. S. Sahni, in *Phase Transitions and Critical Phenomena*, edited by C. Domb and J. L. Lebowitz (Academic Press, London, 1983), Vol. 8, p. 267.

[4] A. J. Bray, Adv. Phys. **43**, 357 (1994).

[5] S. Dattagupta and S. Puri, *Dissipative Phenomena in Condensed Matter: Some Applications* (Springer, Berlin, 2004).

[6] *Dynamics of Ordering Processes in Condensed Matter*, edited by S. Komura and H. Furukawa (Plenum Press, New York, 1988).

[7] R. A. L. Jones, L. J. Norton, E. J. Kramer, F. S. Bates, and P. Wiltzius, Phys. Rev. Lett. **66**, 1326 (1991).

[8] S. Puri and K. Binder, Phys. Rev. A **46**, R4487 (1992); Phys. Rev. E **49**, 5359 (1994).

[9] G. Brown and A. Chakrabarti, Phys. Rev. A **46**, 4829 (1992).

[10] S. Puri and K. Binder, J. Stat. Phys. **77**, 145 (1994).

[11] G. Krausch, Mater. Sci. Eng. R. **14**, 1 (1995).

[12] S. Puri and H. L. Frisch, J. Phys.: Condens. Matter **9**, 2109 (1997).

[13] K. Binder, J. Non-Equilib. Thermodyn. **23**, 1 (1998).

[14] S. Puri and K. Binder, Phys. Rev. Lett. **86**, 1797 (2001); Phys. Rev. E **66**, 061602 (2002).

[15] S. Bastea, S. Puri, and J. L. Lebowitz, Phys. Rev. E **63**, 041513 (2001).

[16] J. M. Geoghegan and G. Krausch, Prog. Polym. Sci. **28**, 261 (2003).

[17] S. Puri, J. Phys.: Condens. Matter **17**, R101 (2005).

[18] S. K. Das, S. Puri, J. Horbach, and K. Binder, Phys. Rev. E **72**, 061603 (2005).

[19] S. K. Das, S. Puri, J. Horbach, and K. Binder, Phys. Rev. Lett. **96**, 016107 (2006); Phys. Rev. E **73**, 031604 (2006).

[20] K. Binder and H. L. Frisch, Z. Phys. B: Condens. Matter **84**, 403 (1991).

[21] K. Binder, in *Phase Transitions and Critical Phenomena*, edited by C. Domb and J. L. Lebowitz (Academic Press, London, 1983) Vol. 8, p. 1.

[22] H. W. Diehl, in *Phase Transitions and Critical Phenomena*, edited by C. Domb and J. L. Lebowitz (Academic Press, London, 1986), Vol. 10, p. 75.

[23] J. W. Cahn, J. Chem. Phys. **66**, 3667 (1977).

[24] M. E. Fisher, J. Stat. Phys. **34**, 667 (1984); J. Chem. Soc., Faraday Trans. 2 **82**, 1569 (1986).

[25] P. G. de Gennes, Rev. Mod. Phys. **57**, 827 (1985).

[26] D. E. Sullivan and M. M. Telo da Gama, in *Fluid Interfacial Phenomena*, edited by C. A. Croxton (Wiley, New York, 1986) p. 45.

[27] S. Dietrich, in *Phase Transitions and Critical Phenomena*, edited by C. Domb and J. L. Lebowitz (Academic Press, London, 1988) Vol. 12, p. 1.

[28] M. Schick, in *Liquids at Interfaces*, edited by J. Charvolin, J.-F. Joanny, and J. Zinn-Justin (North-Holland, Amsterdam, 1990) p. 415.

[29] K. Binder, D. P. Landau, and M. Müller, J. Stat. Phys. **110**, 1411 (2003).

[30] D. M. Kroll and G. Gompper, Phys. Rev. B **39**, 433 (1989).

[31] K. Binder and D. P. Landau, J. Chem. Phys. **96**, 1444 (1992).

[32] M. E. Fisher and H. Nakanishi, J. Chem. Phys. **75**, 5857 (1981).

[33] R. Evans, J. Phys.: Condens. Matter **2**, 8989 (1990).

[34] L. D. Gelb, K. E. Gubbins, R. Radhakrishnan, and M. Sliwinska-Bartkowiak, Rep. Prog. Phys. **62**, 1573 (1999).

[35] M. Müller, K. Binder, and E. V. Albano, Physica A **279**, 188 (2000); Int. J. Mod. Phys. B **15**, 1867 (2001).

[36] M. Müller, K. Binder, and E. V. Albano, Europhys. Lett. **50**, 724 (2000).

[37] M. Müller and K. Binder, J. Phys.: Condens. Matter **17**, S333 (2005).

[38] P. C. Hohenberg and B. I. Halperin, Rev. Mod. Phys. **49**, 435 (1977).

[39] I. Schmidt and K. Binder, Z. Phys. B: Condens. Matter **67**, 369 (1987).

[40] K. Binder, Z. Phys. **267**, 313 (1974).

[41] K. Kawasaki, in *Phase Transitions and Critical Phenomena*, edited by C. Domb and M. S. Green (Academic Press, London, 1972) Vol 2, Chap. 11.

[42] I. C. Henderson and N. Clarke, Macromol. Theory Simul. **14**, 435 (2005).

[43] J.-I. Fukuda, M. Yoneya, and H. Yokoyama, Phys. Rev. E **73**, 066706 (2006).

[44] J. G. Amar, F. E. Sullivan, and R. D. Mountain, Phys. Rev. B **37**, 196 (1988).

[45] R. J. Glauber, J. Math. Phys. **4**, 294 (1963).

[46] I. M. Lifshitz and V. V. Slyozov, J. Phys. Chem. Solids **19**, 35 (1961).